

# Voltammetric behaviour of platinum in aqueous solutions containing sodium hypophosphite

J. J. PODESTÁ, R. C. V. PIATTI, A. J. ARVIA\*

*Instituto de Investigaciones Fisicoquímicas Teóricas y Aplicadas (INIFTA), Facultad de Ciencias Exactas, Universidad Nacional de La Plata, Sucursal 4, Casilla de Correo 16, (1900) La Plata, Argentina*

Received 22 November 1988; revised 20 June 1989

The anodic and cathodic behaviour of polycrystalline Pt in sodium hypophosphite solutions has been investigated by cyclic voltammetry. In acid solutions the voltammograms show that, owing to the presence of the reducing agent, electrooxidation of species related to  $\text{H}_3\text{PO}_3$  occurs in the potential range 0.6 to 1.4 V with respect to NHE. In alkaline solutions the presence of  $\text{NaH}_2\text{PO}_2$  partially inhibits the HER and displaces the formation of the oxygen monolayer on platinum to higher potentials. The voltammetric peaks are attributed to the electrooxidation of the products resulting from the chemical decomposition of  $\text{NaH}_2\text{PO}_2$  in contact with the Pt surface.

## 1. Introduction

Techniques for obtaining metallic deposits by the autocatalytic method employing sodium hypophosphite as reducing agent are widely known [1-3]. The electrochemical behaviour of hypophosphite depends strongly on the nature of the metal employed as substrate, operational temperature and bath composition. Previous reports on the electrochemical oxidation of the hypophosphite anion concluded that the reaction on Pt does not occur even at high temperature [4], while others claimed a very low current efficiency [5].

Hypophosphite electrooxidation in sodium citrate solution as complexing agent was investigated on Pt, Au and Ni [6], where anodic currents in the region between  $-1.0$  and  $-0.2$  V w.r.t. SCE were observed, in contrast to Pt where the current increased monotonically from  $-0.5$  V w.r.t. SCE upwards. This difference was assigned to the increasing apparent activation energy for the reaction on the different metals, but it appears that a more critical evaluation of these results is required. Thus, it was suggested that the oxidation of hypophosphite ( $\text{H}_2\text{PO}_2^-$ ) to phosphite ( $\text{H}_2\text{PO}_3^-$ ) which occurs on Pd between  $-0.4$  and  $+0.8$  V w.r.t. NHE, applied to Pt where the current starts at more positive potentials, in spite of the fact that the current efficiency for the reaction on Pt-Pd substrates becomes zero at about  $70^\circ\text{C}$  [7]. On the other hand, recent voltammetric data for Pt in  $0.125$  M  $\text{NaH}_2\text{PO}_2$  exhibit no electrooxidation current for the anion on this substrate [8]. Apparently these discrepancies depend strongly on the solution composition. The fractional reaction orders for hypophosphite electrooxidation ranging from 0.25 to 0.80 [6, 9] suggest that the reaction is complex and involves side reactions such as disproportionation reactions generating P and intermediate products which delay the

oxidation reaction itself, as well as codeposition phenomena and reactions of ligands originated by different complexing agents which also interfere in the main process. It is agreed that the electrochemical oxidation of hypophosphite is a slow reaction which takes place with an appreciable rate at  $80$  to  $90^\circ\text{C}$  on Ni, Pd, C, Pb and  $\text{PbO}_2$  [7].

The importance of electroless metal deposition (EMD) justifies further investigation of the behaviour of hypophosphite as reducing agent on Pt substrates and relating it to the EMD mechanism. If the latter implies that  $\text{H}_{\text{ad}}$  or  $\text{H}_2$  be produced through the catalytic dehydrogenation of aqueous hypophosphite ions, it is difficult to understand why a metal such as Pt, which is a good electrocatalyst for reduction processes through H-adatoms, should be inefficient in EMD. The answers to these question will provide new arguments with respect to the more probable mechanism for EMD from hypophosphite-containing baths, i.e. whether the dehydrogenation mechanism of Brenner and Riddell [1, 2] or the theory of Wagner and Traud [10-15], or the hydride mechanism turns out to be most appropriate [16, 17].

## 2. Experimental

The measurements were made with a three compartment double wall Pyrex glass cell of a conventional design with a Pt polycrystalline (pc) working electrode, a Pt pc counter-electrode, and a hydrogen reference electrode connected through a Luggin capillary. Potentials in the text are given on the NHE scale. The working electrode was made from a pc Pt wire  $0.05$  cm diameter,  $1.5$  cm long ( $0.235$  cm<sup>2</sup> apparent area). The electrode was previously polished to a mirror surface with an  $\text{Al}_2\text{O}_3$ -water suspension, then rinsed with triply distilled water, and subsequently immersed in

\* Author to whom all correspondence should be addressed.

concentrated  $\text{H}_2\text{SO}_4$  at  $50^\circ\text{C}$  for 10 min followed by another rinsing with triply distilled water.

Solutions were prepared from  $0.5\text{ M H}_2\text{SO}_4$  with addition of  $\text{NaOH}$  (base solution) to adjust the solution pH ( $0.55 \leq \text{pH} \leq 11.85$ );  $x\text{ M NaH}_2\text{PO}_2 \cdot 2\text{H}_2\text{O}$  was added in the concentration range  $1 \times 10^{-4} \leq x \leq$

$0.32\text{ M}$ . Solutions were prepared from Millipore water and p.a. chemicals.

Purified  $\text{N}_2$  was passed through the electrolyte solutions for 30 min prior to the electrochemical measurements. Runs were performed at  $25$  and  $80^\circ\text{C}$ .

### 3. Results

Figure 1a shows the voltammograms obtained for  $\text{Pt}/0.5\text{ M H}_2\text{SO}_4$  (pH 0.55) at  $25^\circ\text{C}$  with and without  $0.01\text{ M NaH}_2\text{PO}_2$  addition at  $0.05\text{ V s}^{-1}$ . The voltammogram (dotted line) in the absence of  $\text{NaH}_2\text{PO}_2$ , exhibits hydrogen (HIIa, HIIc, HIC, HIIC) and oxygen (Oa and Oc) electroadsorption peaks. In the presence of  $1 \times 10^{-2}\text{ M NaH}_2\text{PO}_2$ , the voltammogram (full line) presents a large anodic charge between  $0.60$  and  $1.40\text{ V}$  with a very broad peak (PIIa) at around  $1.2\text{ V}$  preceded by a hump at around  $0.80\text{ V}$ . In this case the H-atom charge decreases approximately to one third the value resulting for the blank. The reverse sweep shows an anodic current with a broad peak (PIa) at around  $0.80\text{ V}$ , and the disappearance of peak Oc.

When the sweep rate,  $v$ , is increased to  $0.5\text{ V s}^{-1}$  in the presence of  $\text{NaH}_2\text{PO}_2$  (Fig. 1b, full trace), PIIa increases and its potential is shifted slightly positively. The height of peak PIIa increases with  $v^{1/2}$  in the lower range of  $v$ , but at  $v$  higher than  $0.3\text{ V s}^{-1}$  it grows more rapidly, presumably because of the relatively larger contribution of oxygen electroadsorption, which increases linearly with  $v$ . Under these conditions the charge of peak Oc is approximately around 15% of the monolayer charge ( $0.420\text{ }\mu\text{C cm}^{-2}$ ), and the decrease in the H-atom charge is about 30%. These experiments show that at high  $v$  the oxidation reaction leaves free sites on the Pt surface to allow the partial formation of an O-electroadsorbed species. Likewise, the shift in the potential of peak PIIa is linear with  $\log v$ . In principle, these relationships suggest that the second stage of the electrooxidation reaction becomes diffusion controlled with a certain degree of irreversibility that appears clearer at high  $v$ . In the presence of  $\text{NaH}_2\text{PO}_2$  the potential of peak Oc is independent of  $v$ , but its height increases linearly with  $v$  (Fig. 1b). Similar runs made at  $0.05\text{ V s}^{-1}$  and  $80^\circ\text{C}$  (Fig. 1c) in  $10^{-2}\text{ M NaH}_2\text{PO}_2$  show no H-atom voltammetric charge. Furthermore, peaks PIa and PIIa become very symmetrical and well defined and the hump preceding peak PIIa at low temperatures has now disappeared.

For  $\text{Pt}/0.5\text{ M H}_2\text{SO}_4 + 0.01\text{ M NaH}_2\text{PO}_2$ , pH 1.55 at  $25^\circ\text{C}$  the same voltammetric features are observed. In this case, the influence of the anodic potential limit was change stepwise to identify the possible conjugated redox systems involved in the overall reaction. Thus, at low  $v$  ( $0.05\text{ V s}^{-1}$ ) and low anodic limits (Fig. 2a), peak PIa is almost absent and the H-atom charge is diminished. In turn, when the anodic limit is in the potential range of peak PIIa, the returning potential sweep shows an enhancement of peak PIa and a slight increase in the H-atom charge. The same run made at high  $v$  ( $0.3\text{ V s}^{-1}$ ) (Fig. 2b) also shows a new cathodic

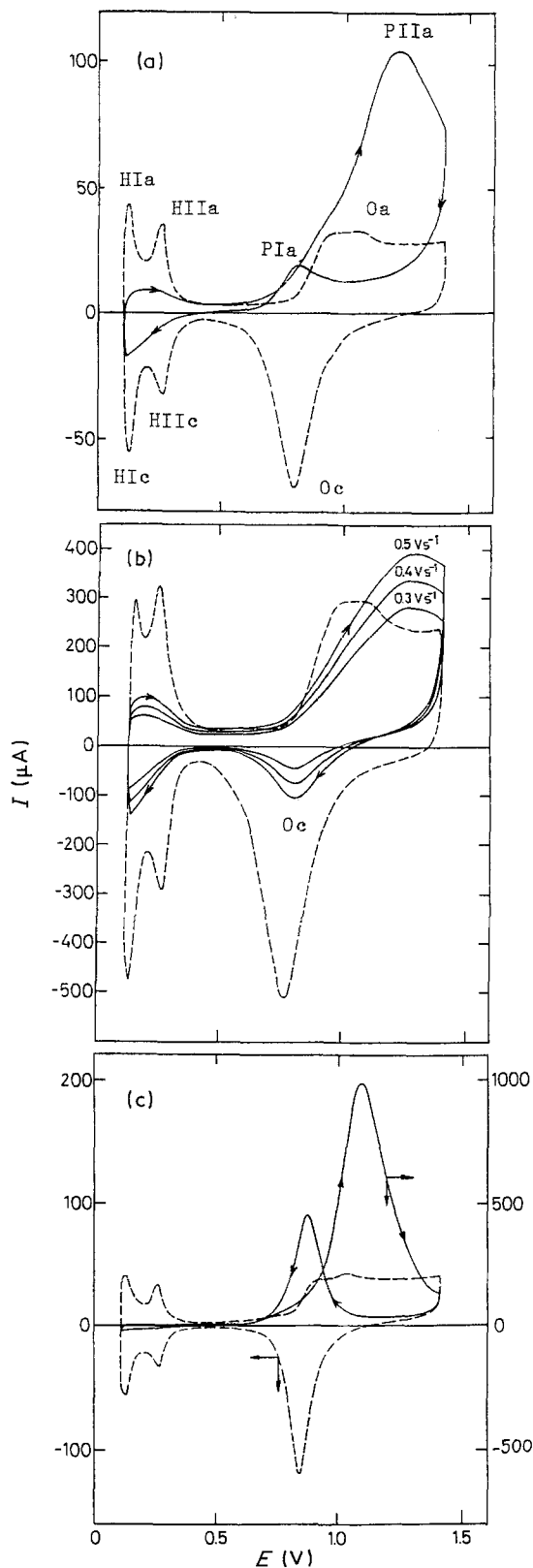


Fig. 1. Voltammograms of a Pt electrode in  $0.5\text{ M H}_2\text{SO}_4$  in the absence (---) and in the presence (—) of  $1 \times 10^{-2}\text{ M NaH}_2\text{PO}_2$  in the bulk solution: (a) pH 0.55,  $25^\circ\text{C}$ ,  $v = 0.05\text{ V s}^{-1}$ ; (b) pH 0.55,  $25^\circ\text{C}$ , sweep rates,  $v$ , indicated on the figure; (c) pH 0.55,  $80^\circ\text{C}$ ,  $v = 0.05\text{ V s}^{-1}$ . Apparent electrode area:  $0.235\text{ cm}^2$ .

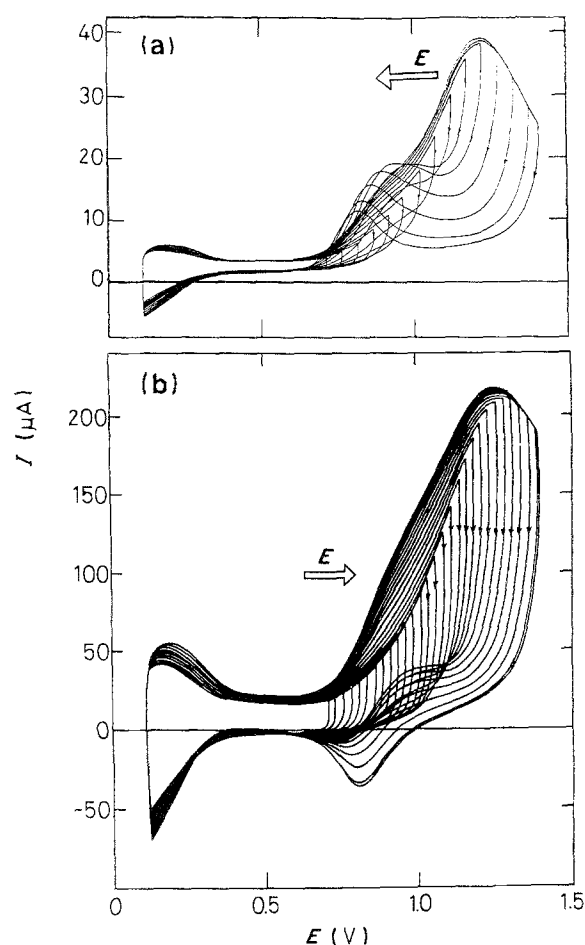


Fig. 2. Repetitive cyclic voltammetry of a Pt electrode in 0.5 M  $\text{H}_2\text{SO}_4 + 1 \times 10^{-2}$  M  $\text{NaH}_2\text{PO}_2$ : (a) pH 1.55, 25°C,  $v = 0.05 \text{ V s}^{-1}$  by gradually decreasing the anodic potential limit at a constant cathodic potential limit; (b) pH 1.55, 25°C,  $v = 0.30 \text{ V s}^{-1}$  by gradually increasing the anodic potential limit at a constant cathodic potential limit. Apparent electrode area:  $0.235 \text{ cm}^2$ .

contribution in the returning scan at around 0.75 V, when the anodic potential limit lies between 1.1 and 1.2 V. All voltammograms in which the H-atom charge can be observed always exhibit an anodic current in the 0.4 to 0.8 V range (Figs 1a, b and 2a, b). For the same system at 80°C (Fig. 3) a relatively small voltammetric current appears for anodic potential limits up to around 1.0 V but as the latter increases the development of peak IIa is noticed. Likewise the returning scan shows the appearance of peak PIa for both low and high values of  $v$ . This peak is shifted more negatively as the anodic potential limit increases. Slight changes in the voltammograms run by changing the anodic potential limits either upwards or downwards can be noticed.

At pH 11.85 and 25°C the presence of  $\text{NaH}_2\text{PO}_2$  (Fig. 4a) modifies the H-atom voltammogram and apparently displaces the O-electrodesorption to higher potentials, but at  $0.5 \text{ V s}^{-1}$  (Fig. 4b) no reaction of  $\text{NaH}_2\text{PO}_2$  itself can be seen. The O-electrodesorption charge is nearly independent of the presence of  $\text{NaH}_2\text{PO}_2$  in solution. In this case, the height of peak Oc varies linearly with  $v$  as expected for the O-electrodesorption/electrodesorption reaction. However, at 80°C (Fig. 5) the O-electrodesorption voltammogram is,

to a large extent, replaced by an anodic peak appearing at near 0.9 V. Furthermore, the returning voltammogram at  $0.03 \text{ V s}^{-1}$  shows an incipient anodic current at about 0.7 V, which cannot be observed at  $0.05 \text{ V s}^{-1}$ .

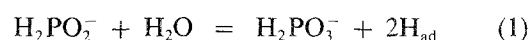
For 0.5 M  $\text{H}_2\text{SO}_4 + 0.01 \text{ M NaH}_2\text{PO}_2$  containing an excess of  $\text{NaH}_2\text{PO}_3$ , pH 0.55 and 80°C, PIa is strongly enhanced for the potential sweep run either anodically or cathodically (Fig. 6). These runs indicate that PIa is associated with the oxidation of  $\text{H}_2\text{PO}_3^-$  to  $\text{H}_3\text{PO}_4$ . Likewise as PIa increases in the returning sweep, PIIa is no longer observed.

At 25°C the voltammograms obtained in the 0 to  $7.5 \times 10^{-3}$  M  $\text{NaH}_2\text{PO}_2$  range show almost linear increase in the height of PIIa and a gradual decrease in the H-atom charge with the  $\text{NaH}_2\text{PO}_2$  concentration up to  $1 \times 10^{-3}$  M (Fig. 7), whereas for concentrations higher than  $5 \times 10^{-3}$  M, the height of PIIa approaches a limiting value and, correspondingly, a limiting oxidation charge. The dependence of the height of PIIa with  $\text{NaH}_2\text{PO}_2$  concentration can be seen in Fig. 8. The saturation charge density of peak PIIa is  $325 \mu\text{C cm}^{-2}$ , that is approximately 4.5 times greater than the charge density derived from peak Oc. The electrooxidation of  $\text{NaH}_2\text{PO}_2$  (0.32 M, pH 0.55) (Fig. 9) shows that peak Oc only appears at higher values of  $v$ , whereas peak PIIa appears at lower values of  $v$ . A linear dependence of the height of peak PIIa on  $v^{1/2}$  is observed (Fig. 10). In this case, when the oxidation scan includes a potential holding at 1.35 V (Fig. 11), PIIa is strongly depressed for potential holding times ranging from 60 to 180 s. This fact can be related either to an interference of the product from the chemical oxidation of  $\text{H}_2\text{PO}_2^-$  accumulated at the interface, namely  $\text{H}_2\text{PO}_3^-$ , gradually goes into solution as the potential holding time increases, or to the chemical oxidation of  $\text{H}_2\text{PO}_2^-$  itself, which progressively inhibits the Pt electrode for the anodic reactions.

#### 4. Discussion

Results indicate that peaks PIa and PIIa correspond to the electrooxidation of products from the chemical decomposition of  $\text{NaH}_2\text{PO}_2$  on the Pt surface. The  $\text{H}_2\text{PO}_2^-$  anion is electrooxidized at relatively large negative potentials on certain substrates where the efficiency of EMD is very high. For these materials, that is Ni, Pd, C, etc., the existence of a large surface concentration of H-atoms appears to be unlikely, as evident from inspection of the mechanisms of the HER on different metals discussed in the literature [18].

According to previous studies [1, 2] the equilibrium



is established on Pt in contact with a  $\text{NaH}_2\text{PO}_2$  solution. This reaction can be shifted to the right provided that the fast desorption of H-atoms as molecular hydrogen can occur



The voltammetric currents associated with the HER

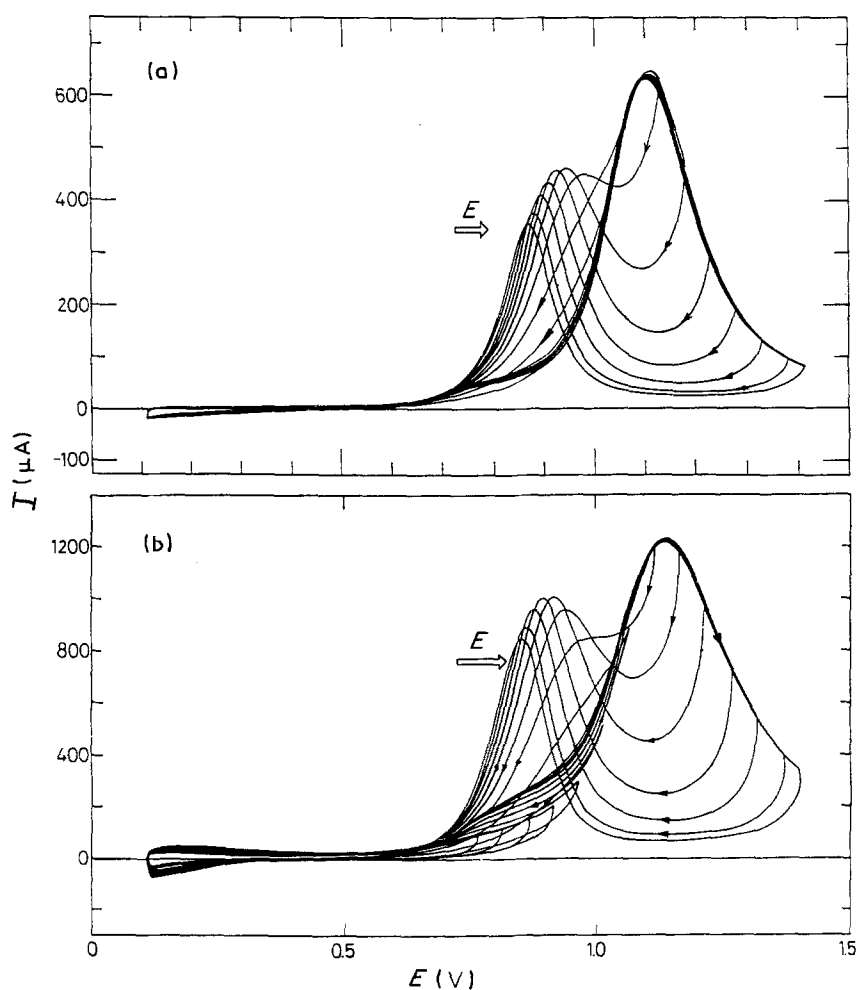


Fig. 3. Repetitive cyclic voltammetry of a Pt electrode in 0.5 M  $\text{H}_2\text{SO}_4 + 1 \times 10^{-2}$  M  $\text{NaH}_2\text{PO}_2$ , pH 1.55, 80°C, by gradually increasing the anodic potential limit at a constant cathodic potential limit: (a)  $v = 0.05 \text{ V s}^{-1}$ ; (b)  $v = 0.30 \text{ V s}^{-1}$ . Apparent electrode area:  $0.235 \text{ cm}^2$ .

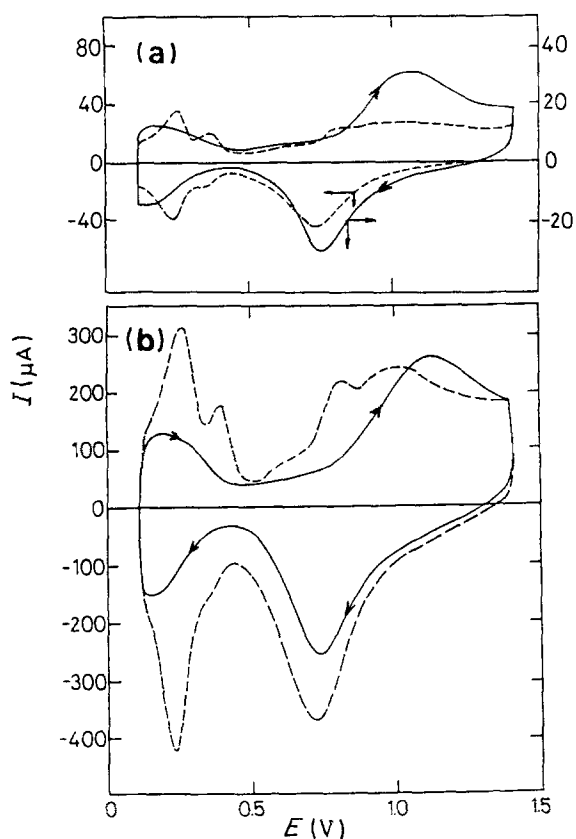


Fig. 4. Voltammograms of a Pt electrode in 0.5 M  $\text{Na}_2\text{SO}_4$  in the absence (---) and in the presence (—) of  $1 \times 10^{-2}$  M  $\text{NaH}_2\text{PO}_2$  in the bulk of solution, pH 11.85, 25°C: (a)  $v = 0.05 \text{ V s}^{-1}$ ; (b)  $v = 0.50 \text{ V s}^{-1}$ . Apparent electrode area:  $0.235 \text{ cm}^2$ .

can be observed at potentials ranging from 0 to 0.4 V at low (25°C) and high (80°C) temperatures. The increase in peak PIIa gradually inhibits the HER itself although no complete inhibition of this reaction can be achieved. This indicates that Reaction 1 prevails on Pt in the vicinity of the hydrogen electrode potential value. Nevertheless, the occurrence of Reaction 1 does not necessarily imply that EMD becomes enhanced. This conclusion is opposed to those reaction mechanisms where it is assumed that H-adatoms play an important role in EMD. If this were the case, the voltammetric peaks PIa and PIIa could be wrongly assigned to direct electrooxidation reactions involving  $\text{H}_2\text{PO}_2^-$  ions. The fact that the height of peak PIa appears to be almost independent of  $\text{NaH}_2\text{PO}_2$  concentration, whereas that of peak PIIa depends on the square root of  $\text{NaH}_2\text{PO}_2$  concentration, can be explained on the basis of Reaction 1 by further admitting that it produced coadsorbed  $\text{H}_2\text{PO}_3^-$  ions and H-adatoms on the Pt surface. Otherwise, the fact that in acid solution peak PIa appears clearer than in alkaline solution can be interpreted through  $\text{H}_2\text{PO}_2^-$  ion oxidation, in the potential range of peak PIa, yielding the local formation of  $\text{H}_3\text{PO}_4$  in acid according to the reaction



but in alkaline solution  $\text{PO}_4^{3-}$  ions are formed accord-

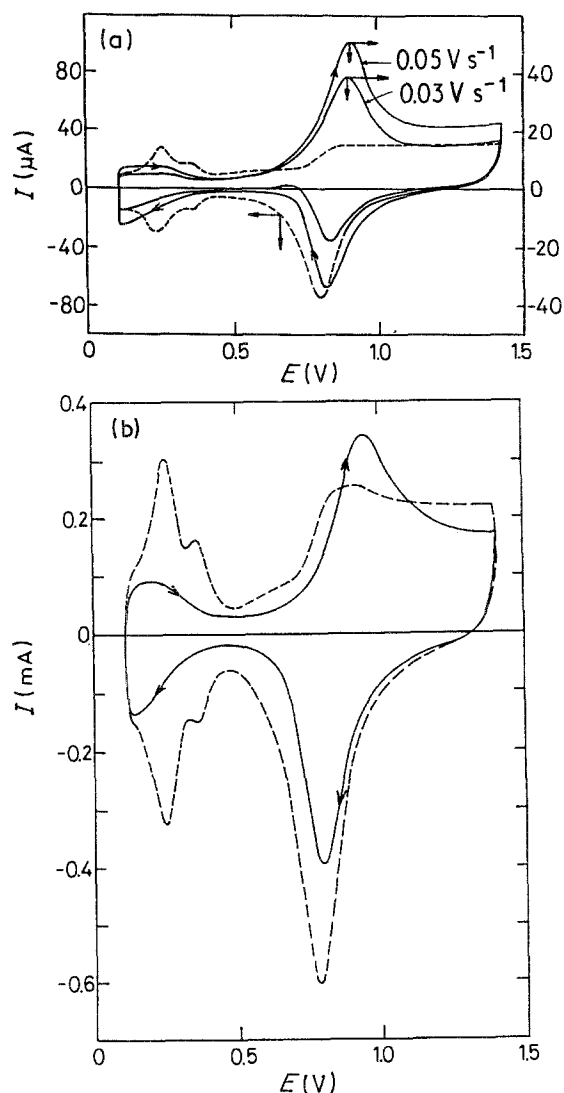
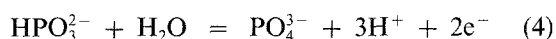


Fig. 5. (a) Voltammograms of a Pt electrode in base solution in the absence (---) and in the presence (—) of  $1 \times 10^{-2}$  M  $\text{NaH}_2\text{PO}_2$  in the bulk solution, pH 11.85,  $80^\circ\text{C}$ . Sweep rates,  $v$ , indicates in the figure. Apparent electrode area:  $0.235\text{ cm}^2$ . (b) Voltammograms of a Pt electrode in base solution in the absence (---) and in the presence (—) of  $1 \times 10^{-2}$  M  $\text{NaH}_2\text{PO}_2$  in the bulk solution, pH 11.85,  $80^\circ\text{C}$ ,  $v = 0.50\text{ V s}^{-1}$ . Apparent electrode area:  $0.235\text{ cm}^2$ .

ing to



In acid solution peak PIa appears at approximately 0.8 V. Recently FTIR studies on the Pt/ $\text{H}_3\text{PO}_4$  system confirm that the maximum surface coverage of Pt by  $\text{H}_3\text{PO}_4$  is attained at 0.8 V [19]. Therefore, the  $\text{H}_3\text{PO}_3$  electrooxidation reaction can be inhibited by the adsorption of the reaction product on the electrode surface. Hence, it is reasonable to assign peak PIa to an electrochemical reaction taking place on a Pt surface covered mainly by adsorbed  $\text{HPO}_3^{2-}$  ions, the product of the reaction being adsorbed  $\text{H}_3\text{PO}_4$ .

The second adsorbed stage of  $\text{H}_3\text{PO}_3$  on Pt in acid appears when the potential is set more positive than 0.8 V. Then the inhibition caused by  $\text{H}_3\text{PO}_4$  decreases, and fresh Pt surface becomes available for further electrooxidation of  $\text{H}_3\text{PO}_3$ , the latter resulting from Reaction 1 and its equilibrium in solution. This situation leads to reaction kinetics under diffusion

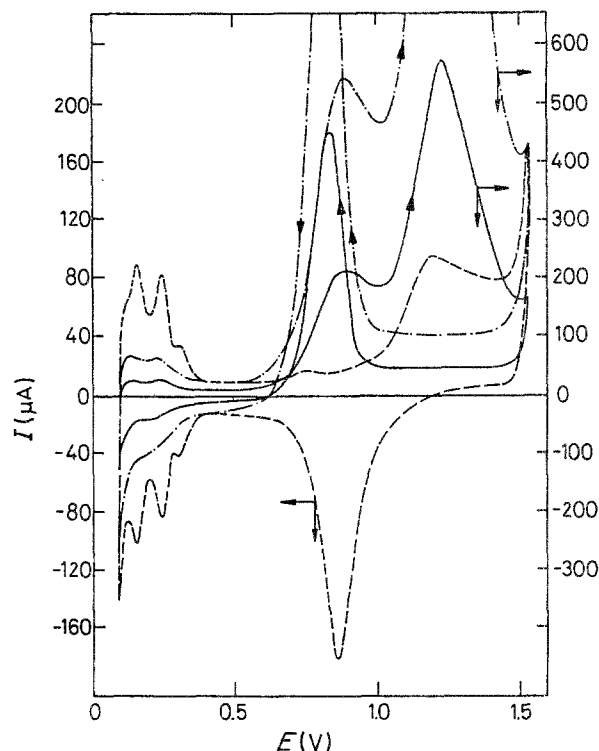


Fig. 6. Voltammograms of a Pt electrode in  $0.5\text{ M H}_2\text{SO}_4$  in the absence (---) and in the presence (—) of  $1 \times 10^{-2}$  M  $\text{NaH}_2\text{PO}_2$  in the bulk of solution. pH 0.55,  $80^\circ\text{C}$ ,  $v = 0.20\text{ V s}^{-1}$ . (.....)  $\text{Na}_2\text{HPO}_3$  addition. Apparent electrode area:  $0.235\text{ cm}^2$ .

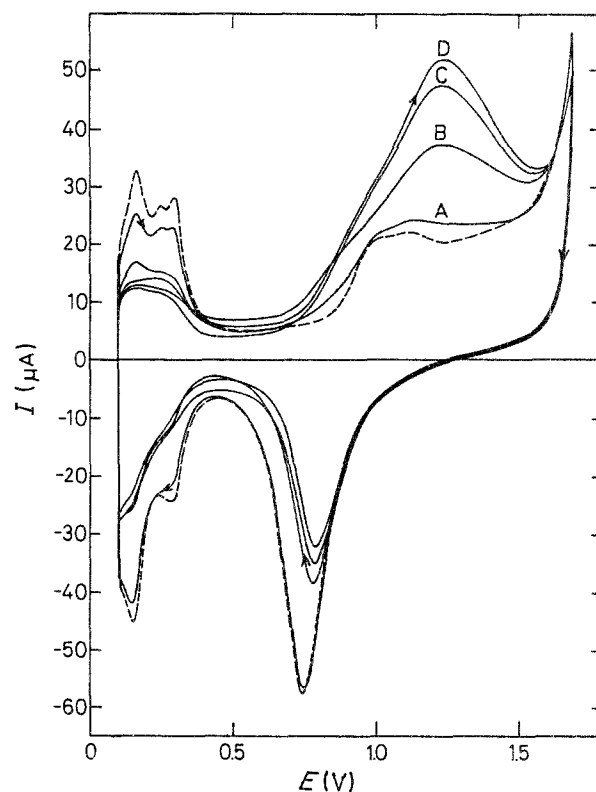


Fig. 7. Voltammograms of a Pt electrode in  $0.5\text{ M H}_2\text{SO}_4$  in the absence (---) and in the presence (—) of different  $\text{NaH}_2\text{PO}_2$  concentrations: A  $1 \times 10^{-4}$  M; B  $1 \times 10^{-3}$  M; C  $0.5 \times 10^{-3}$  M; D  $7.5 \times 10^{-3}$  M;  $v = 0.10\text{ V s}^{-1}$ . Apparent electrode area:  $0.235\text{ cm}^2$ .

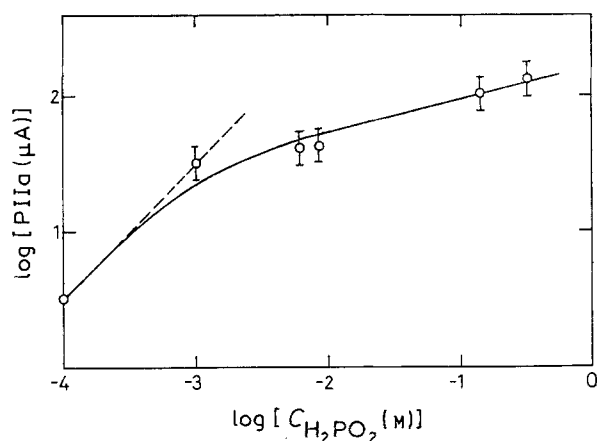


Fig. 8. Plot of log PIIa against log  $\text{NaH}_2\text{PO}_2$  concentration. Data taken from Fig. 7.

control. Otherwise, in alkaline solution because free  $\text{H}_3\text{PO}_4$  neither exists nor is formed throughout  $\text{HPO}_3^{2-}$  oxidation, the electrooxidation reaction proceeds directly to  $\text{PO}_4^{3-}$ . This reaction corresponds to peak PIIa and, according to Reaction 4, one can expect that adsorbed  $\text{HPO}_3^{2-}$  coexists with O-adatoms.

From the charge density balance, neglecting a constant roughness factor correction, one can attempt to discriminate from the voltammetric data the possible composition of the adsorbed monolayer. Thus, in the absence of  $\text{NaH}_2\text{PO}_2$  addition the O-adatom charge density is  $1.44 \text{ mC cm}^{-2}$ , the total anodic charge density in the presence of  $\text{NaH}_2\text{PO}_2$  is  $1.68 \text{ mC cm}^{-2}$ , and for the latter, the O-adatom charge density is  $0.464 \text{ mC cm}^{-2}$ . Hence, the net charge density that can be assigned to adsorbed  $\text{H}_3\text{PO}_3$  is  $1.22 \text{ mC cm}^{-2}$ . From these values the Pt surface sites appear to be distributed one third for O-adatom and the rest for  $\text{H}_3\text{PO}_3$  adsorbates. This is consistent with the fact that each  $\text{H}_3\text{PO}_3$  occupies at least two Pt surface sites.

Under the conditions described in Fig. 2a the entire

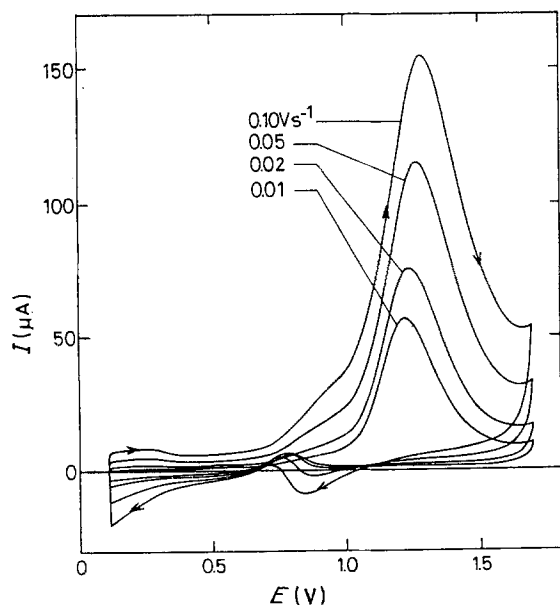


Fig. 9. Effect of potential sweep rate on cyclic voltammograms of a Pt electrode in  $0.5 \text{ M H}_2\text{SO}_4 + 0.32 \text{ M NaH}_2\text{PO}_2$  solution, pH 0.55,  $25^\circ \text{C}$ . Sweep rates,  $v$ , indicates in the figure. Apparent electrode area:  $0.235 \text{ cm}^2$ .

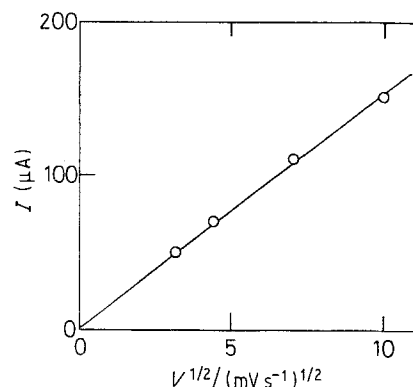


Fig. 10. Dependence of current peak PIIa on  $v^{1/2}$ . Data taken from Fig. 9.

voltammogram exhibits an anodic current component which can be attributed to the continuous electrooxidation of hydrogen and generation of  $\text{H}_2\text{PO}_3$  or  $\text{HPO}_3^{2-}$  from 0 V up to the potential range of peak PIa. Accordingly, at low  $v$  the formation of  $\text{H}_3\text{PO}_3$  or  $\text{HPO}_3^{2-}$  inhibits the O-atom electroadsorption on Pt, whereas at high  $v$  the Pt surface coverage by the inhibitor gradually decreases as  $v$  increases. For the latter the reactant at the interface cannot be immediately replenished so that part of the Pt surface is then available for the O-atom electroadsorption. Then, the formation of a surface layer of O-atoms takes place when the potential reaches a value more positive than the potential of peak PIIa.

#### Acknowledgements

This research project was supported financially by the Consejo Nacional de Investigaciones Científicas y Técnicas and the Comisión de Investigaciones Científicas de la Provincia de Buenos Aires (CIC). R.C.V.P. is member of the Professional Career of CIC. The authors thank Ing. C. Yamashiro for his collaboration in the experimental work.

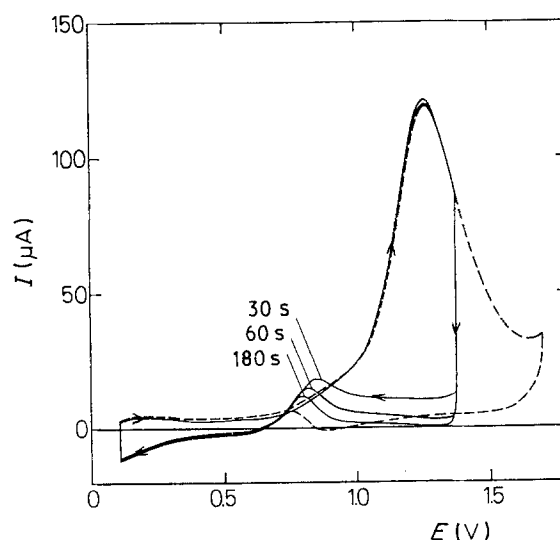


Fig. 11. Voltammograms of a Pt electrode in  $0.5 \text{ M H}_2\text{SO}_4 + 0.32 \text{ M NaH}_2\text{PO}_2$  solution, pH 0.55,  $25^\circ \text{C}$ ,  $v = 0.05 \text{ V s}^{-1}$ . Potential step at 1.35 V during 30, 60 and 180 s. Apparent electrode area:  $0.235 \text{ cm}^2$ .

## References

- [1] A. Brenner and G. E. Riddell, *Proc. Am. Electroplaters Soc.* **33** (1946) 23; *ibid.* **34** (1947) 156.
- [2] *Idem*, *J. Res. Nat. Bur. Standards* **37** (1946) 31; *ibid.* **39** (1947) 385.
- [3] F. A. Lowenheim (Ed.) 'Modern Electroplating', Wiley, New York (1974).
- [4] J. A. Marshall, *J. Electrochem. Soc.* **130** (1983) 369.
- [5] A. P. Tomilov and N. E. Chomutov, 'Encyclopedia of Electrochemistry of the Elements' (Edited by A. J. Bard), Vol. III, Marcel Dekker, New York (1975) p. 27.
- [6] I. Ohno, O. Wakabayashi and S. Haruyama, *J. Electrochem. Soc.* **132** (1985) 2323.
- [7] A. Hickling and D. Johnson, *J. Electroanal. Chem.* **13** (1967) 100.
- [8] J. Flis and D. J. Duquette, *J. Electrochem. Soc.* **131** (1984) 254.
- [9] G. Bech-Nielsen, C. Qvist Jessen and J. C. Reeve, 36 ISE Meeting, Extended Abstracts, Salamanca, Spain (1985) p. 5610.
- [10] C. Wagner and W. Traud, *Z. Elektrochem.* **44** (1938) 391.
- [11] M. Saito, *J. Metal Finishing Soc. Jpn* **16** (1965) 300; *ibid.* **17** (1966) 14.
- [12] M. Paunovic, *Plating* **55** (1968) 1161.
- [13] Y. Okinaka, *J. Electrochem. Soc.* **120** (1973) 739.
- [14] I. Ohno, *Surf. Technol.* **4** (1976) 515.
- [15] C. E. Yamashiro, J. J. Podestá and A. J. Arvia, *Anal. Asoc. Quím. Arg.* **74** (1986) 119.
- [16] R. M. Lukes, *Plating* **51** (1964) 969.
- [17] T. V. Ivanovskaya and K. M. Gorbunova, *Zash. Met.* **2** (1966) 477.
- [18] K. J. Vetter, 'Elektrochemische Kinetik', Springer, Berlin-Göttingen-Heidelberg (1961) p. 432.
- [19] M. A. Habib and J. O'M. Bockris, *J. Electrochem. Soc.* **130** (1983) 2510.